

PAPER • OPEN ACCESS

Magnetocaloric effect in TbCo-based multilayers

To cite this article: A Svalov *et al* 2019 *J. Phys.: Conf. Ser.* **1389** 012101

View the [article online](#) for updates and enhancements.



IOP | ebooks™

Bringing together innovative digital publishing with leading authors from the global scientific community.

Start exploring the collection—download the first chapter of every title for free.

Magnetocaloric effect in TbCo-based multilayers

A Svalov¹, I Makarochkin¹, E Kudryukov¹, E Stepanova¹, V Vas'kovskiy^{1,2}, A Larrañaga³, and G Kurlyandskaya^{1,4}

¹ Ural Federal University, Institute of Natural Sciences and Mathematics, 620002 Ekaterinburg, Russia

² Institute of Metal Physics, Ural Branch of Russian Academy of Sciences, 620108 Ekaterinburg, Russia

³ Universidad del País Vasco (UPV/EHU), Servicios Generales de Investigación, 48940 Bilbao, Spain

⁴ Universidad del País Vasco (UPV/EHU), Departamento de Electricidad y Electrónica and BCMaterials, 48940 Bilbao, Spain

E-mail: andrey.svalov@urfu.ru

Abstract. TbCo-based magnetic multilayers with different thicknesses of Tb-Co layers and non-magnetic spacers (Ti, Si) have been prepared by sputtering. The structure and magnetocaloric properties of these samples have been investigated. The peak value of magnetic entropy change in TbCo-based multilayers is smaller than the one previously reported for bulk counterparts. Nanostructuring leads to a table-like temperature dependence of the magnetic entropy change. It has been shown that the material of non-magnetic spacers can have a noticeable effect on magnetocaloric properties of TbCo-based magnetic multilayers.

1. Introduction

Magnetocaloric effect (MCE) is a subject of special interest, because magnetic refrigeration offers considerable reduction of the operating cost, it is an environmentally friendly alternative to modern refrigerators and air conditioners [1]. For characterization of the magnetocaloric effect (MCE), two important parameters were used. The first one is the magnetic entropy change (ΔS_M) and the second parameter is the refrigeration capacity, which can be defined as the product of the maximum value of the peak of magnetic entropy change ($\Delta S_{M(\max)}(T, H)$) and the width of ΔS_M peak at its half-height [1]. For magnetic cooling over the so-called Ericsson cycle, the ideal material must have both constant and high ΔS_M value throughout the entire working temperature range [2]. Magnetocaloric material in the form of thin films has additional advantage - a high surface-to-volume ratio, which contributes to an increase in the efficiency of heat transfer [3].

Gadolinium remains to be the benchmark for magnetocaloric materials, this explains the interest in the study of MCE features in Gd films and Gd-based multilayers [4–8]. At the same time, Gd-Co amorphous alloys show high refrigeration capacity [9, 10]. In addition, the Curie temperature (T_C) of amorphous ferrimagnetic alloys, and, consequently, the temperature range where the MCE maximum is observed, can be changed by varying their chemical composition. However, thin films allow additional adjustment of the value of T_C , since the magnetic properties of thin films in the nanometer thickness range strongly depend on their thickness [11–13]. In addition, the material of non-magnetic



spacers can also have a noticeable effect on the magnetic properties of rare earth–transition metal multilayers [13]. It should also be noted that in recent years, the search for promising MCE materials has shifted toward composite materials [10, 14]. From this point of view, the use of multilayered structures also seems promising. Replacement the Gd by other rare earth metals such as Tb, Dy can contribute to understanding of characteristics of MCE of rare earth-transition metal amorphous alloys in more details.

In this paper, the magnetic and magnetocaloric properties were comparatively analysed for the case of $[\text{Tb-Co}(3 \text{ nm})/\text{Ti}(2 \text{ nm})]_{30}$ and $[\text{Tb-Co}(6 \text{ nm})/\text{Si}(2 \text{ nm})]_{20}$ nanoscale multilayers prepared by rf-sputtering.

2. Experimental

The Tb-Co-based multilayered structures were prepared by rf-sputtering deposition of Tb-Co layers and Ti or Si spacers onto glass substrates at room temperature for an Ar pressure value of 1.3×10^{-3} mbar. The background vacuum pressure prior to deposition was 5×10^{-7} mbar. The deposition rates were previously calculated on the base of the results of calibration: 0.064 nm/s for Tb-Co, 0.051 nm/s for Ti and Si. A mosaic target was used for preparation of the Tb-Co layers. The compositional ratio of Tb and Co in the Tb-Co layers was determined by X-ray fluorescence spectroscopy. Chemical composition of Tb-Co films deposited using this target was $\text{Tb}_{27}\text{Co}_{73}$. This composition was selected in order to avoid the appearance of magnetic compensation state in the Tb-Co layers in the temperature interval under consideration [15]. Technological magnetic field of 10 mT was applied during deposition in order to induce magnetic anisotropy in plane of the film. The structure of multilayers was studied by X-ray diffraction (XRD) using a PHILIPS X'PERT PRO automatic diffractometer operating with Cu-K α radiation. Low angle X-ray diffraction regime was employed in order to determine the quality of the multilayers. The magnetic properties of the samples were measured by a Quantum Design SQUID magnetometer (MPMS XL7). The magnetic entropy change $\Delta S_M(H, T)$ was quantified using the Maxwell relation.

3. Results and discussion

According to X-ray diffraction evaluation, all investigated multilayers are fully amorphous. The low angle XRD patterns for all multilayers showed well-defined Bragg peaks associated with their periodic structure. Figure 1 shows the low angle X-ray diffraction spectra for $[\text{Tb-Co}(3 \text{ nm})/\text{Ti}(2 \text{ nm})]_{30}$ and $[\text{Tb-Co}(6 \text{ nm})/\text{Si}(2 \text{ nm})]_{20}$ nanoscale multilayers. The presence of good quality XRD peaks even for the samples with 3 nm thickness of Tb-Co layers confirms the existence of a well-defined layered structure in both of the studied cases. Observed peaks allow the determination of the layer thickness, which agrees well with those expected from the deposition time using calibrated deposition rate.

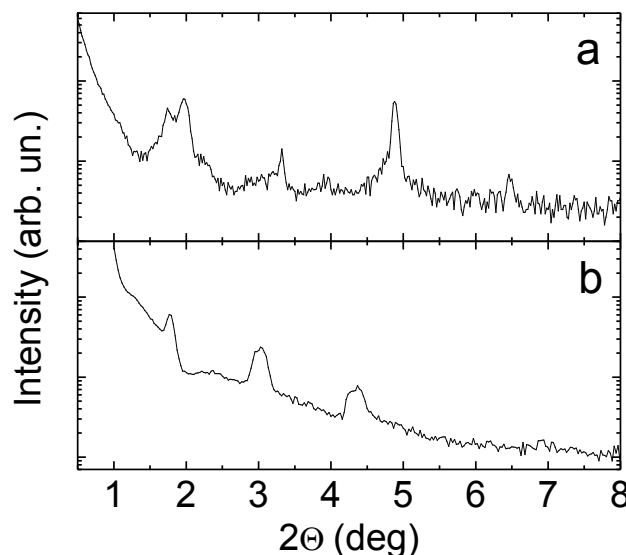


Figure 1. Low-angle X-ray diffractograms for the $[\text{Tb-Co}(3 \text{ nm})/\text{Ti}(2 \text{ nm})]_{30}$ (a) and $[\text{Tb-Co}(6 \text{ nm})/\text{Si}(2 \text{ nm})]_{20}$ (b) multilayer samples.

Figure 2(a) shows the temperature dependence of the magnetization, $M(T)$, for [Tb-Co(3 nm)/Ti(2 nm)]₃₀ sample measured under an applied magnetic field of 10 mT after zero field cooling (ZFC) procedure. The Curie temperature, $T_C \approx 157$ K, was estimated from the $M(T)$ dependence as the minimum of the dM/dT versus T variation (see inset). The strongly diffused minimum of the dM/dT suggests that there is a magnetic non-uniformity in the Tb-Co layers and the existence of a set of phases with a different T_C value. The reason for this can be both the finite-size effect, and a decrease in the magnetic moment of the Co sub-lattice by changing the electronic structure of Co atoms due to the electrons of the Ti sublayers (electron charge transfer effect) [12, 15].

The MCE was estimated in terms of the change in magnetic entropy using a set of magnetic isotherms measured over a wide temperature range including the temperature of the magnetic ordering of the sample. Isotherms were measured in increments of 5 degrees. The magnetic field was applied in the plane of the samples and increased up to 7 T. When $T < T_C$, the magnetization demonstrates intensive growth in small fields, followed by a tendency of saturation in the large fields, exhibiting a behavior typical for ferromagnets. As the temperature increases in the interval $T > T_C$, the shape of the $M(H)$ curves tends to be linear, which is typical for paramagnetic state of materials (Fig. 3).

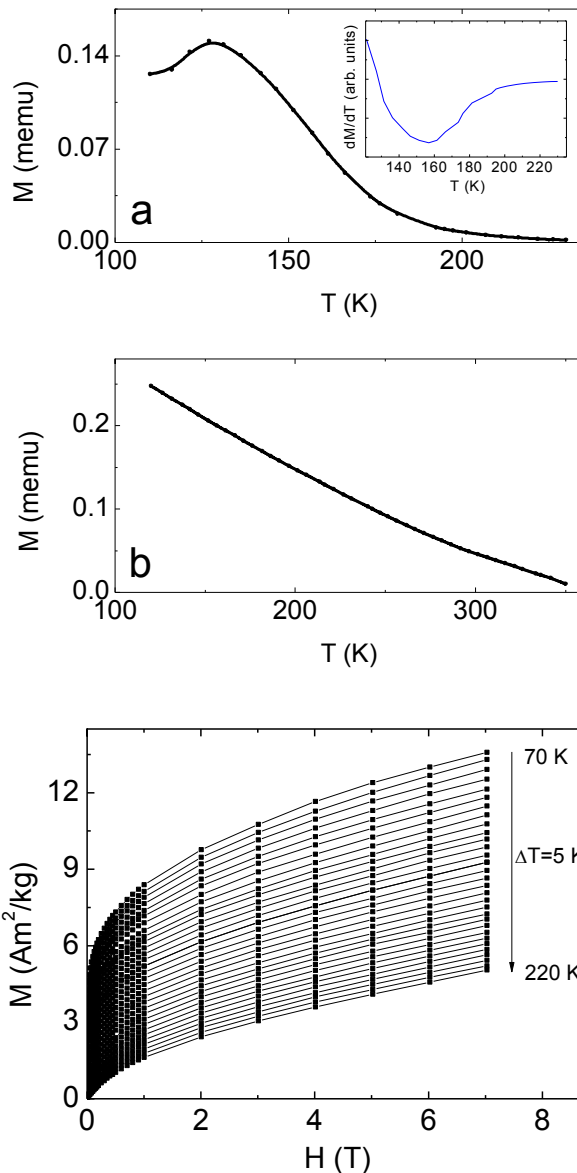


Figure 2. Temperature dependence of the magnetization for the [Tb-Co(3 nm)/Ti(2 nm)]₃₀ (a) and [Tb-Co(6 nm)/Si(2 nm)]₂₀ (b) multilayer samples. The measurements were done on heating with 10 mT applied field after ZFC procedure. Inset: the dM/dT versus T curve.

Figure 3. Magnetization isotherms of the [Tb-Co(3 nm)/Ti(2 nm)]₃₀ multilayers.

The measured M – H isotherms were converted to M^2 versus H/M plots (so-called Belov-Arrrott plots). It can be seen that they are somewhat curved (Fig. 4). As a rule, for homogeneous ferromagnets, the Belov-Arrrott curves are close to the straight lines, and deviations from linearity are usually observed in disordered systems. This can be associated with variations in the strength of exchange bonds [16].

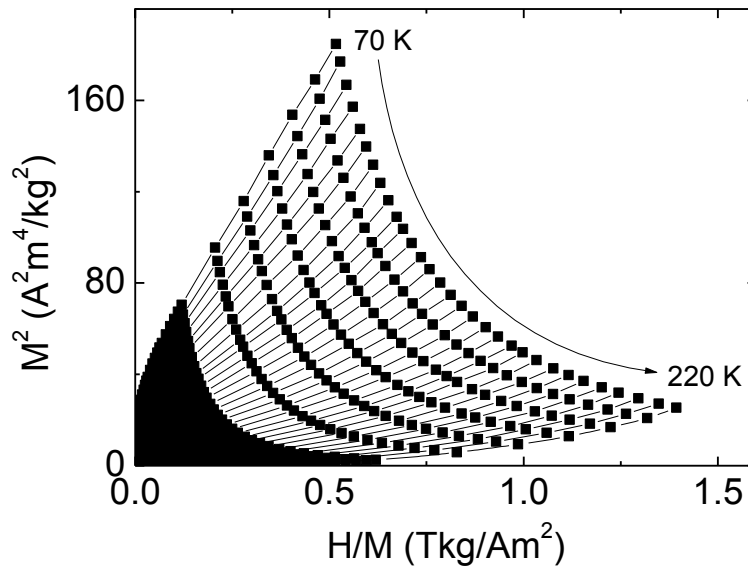


Figure 4. Isothermal M^2 versus H/M plots of the $[\text{Tb-Co}(3 \text{ nm})/\text{Ti}(2 \text{ nm})]_{30}$ multilayers.

The change in magnetic entropy was determined through magnetic isotherms using the Maxwell ratio [17]:

$$\Delta S_M = \int_{H_2}^{H_1} \left(\frac{\partial M}{\partial T} \right)_H dH \quad (1)$$

where ΔS_M – change in magnetic entropy, H - magnetic field, M - magnetization, T - temperature. The maximum of the ΔS_M value in the temperature dependence of the change in magnetic entropy turned out to be 2.2 J/kg·K at $\Delta H = 7$ T (Fig. 5), which is several times lower than for bulk samples [18]. This situation is usually observed in nanostructured materials with respect to their bulk analogues [19]. On the other hand, instead of a sharp peak characteristic for homogeneous magnetic materials with a

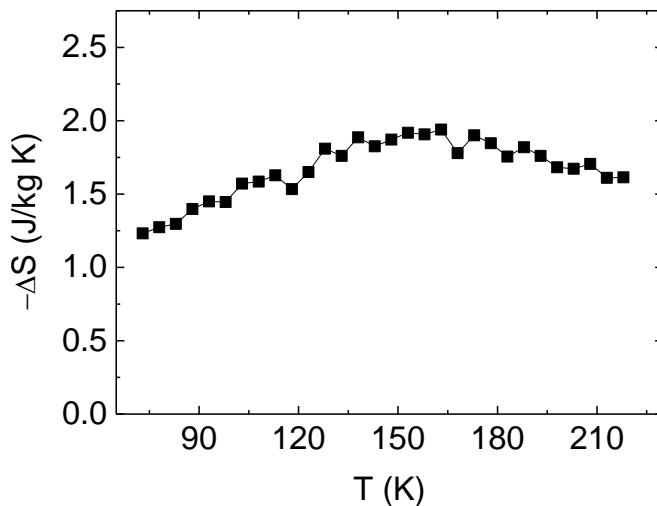


Figure 5. Temperature dependence of magnetic entropy change for the $[\text{Tb-Co}(3 \text{ nm})/\text{Ti}(2 \text{ nm})]_{30}$ multilayers. $\Delta H = 7$ T.

pronounced phase transition temperature, a slight change in ΔS_M is observed in a wide range of temperatures, in the other words, a table-like temperature dependence of the magnetic entropy change takes place. As mentioned above, this ΔS_M behavior is preferable for materials used in magnetic cooling systems operating along the Ericsson cycle.

Figure 2(b) shows the $M(T)$ dependence for $[\text{Tb-Co}(6 \text{ nm})/\text{Si}(2 \text{ nm})]_{20}$. The Curie temperature, $T_C \approx 322 \text{ K}$, was estimated from the $M(T)$ curve by linear extrapolation of the low temperature part to the zero value of M . Taking into account a finite-size effect, an increase of T_C in comparison with $[\text{Tb-Co}(3 \text{ nm})/\text{Ti}(2 \text{ nm})]_{30}$ multilayers seems to be logic as the thickness of the Tb-Co layers is increased by two times.

Fig. 6 shows the magnetic isotherms for $[\text{Tb-Co}(6 \text{ nm})/\text{Si}(2 \text{ nm})]_{20}$ sample. It is seen that there is no abrupt change in the magnetization near the phase transition temperature, which is a sign of a potentially low ΔS_M maximum.

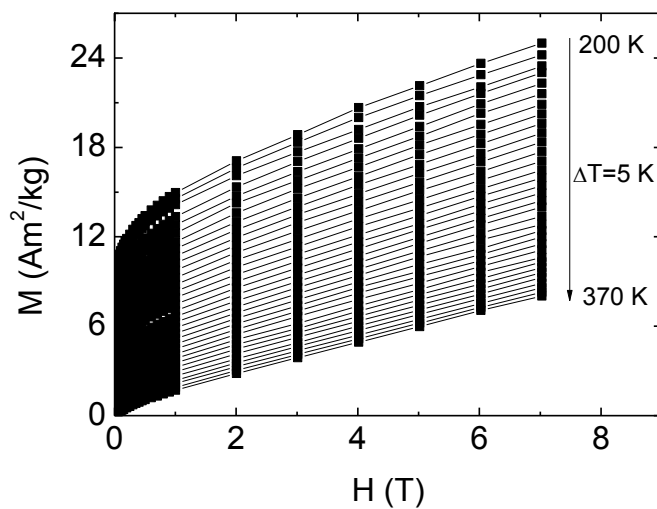


Figure 6. Magnetization isotherms of the $[\text{Tb-Co}(6 \text{ nm})/\text{Si}(2 \text{ nm})]_{20}$ multilayers.

The Belov-Arrott curves for this sample are significantly curved (Fig. 7), indicating a strong magnetic inhomogeneity of the samples. The reason for such behaviour is most likely the properties of the material of the non-magnetic spacer. Silicon is able to diffuse actively into adjacent layers, contributing to the formation of heterogeneous interfaces. In addition, Si actively affects the electronic structure of Co [20]. All above mentioned contributions can cause the appearance of an additional increase of magnetic inhomogeneity of the Tb-Co layers. As a result, the ΔS_M value is greatly reduced (Fig. 8).

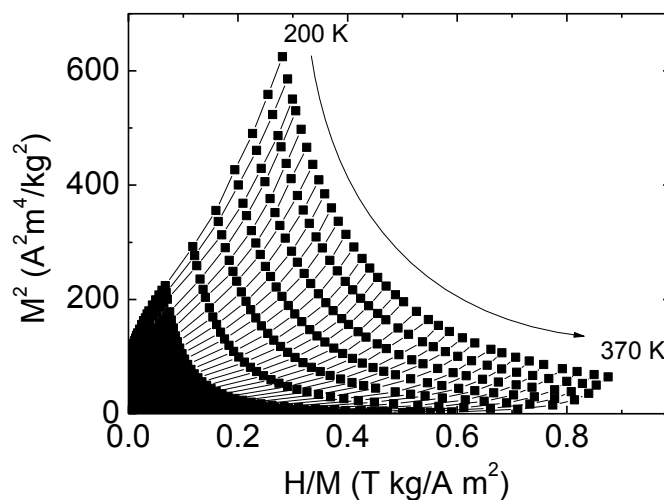


Figure 7. Isothermal M^2 versus H/M plots of the $[\text{Tb-Co}(6 \text{ nm})/\text{Si}(2 \text{ nm})]_{20}$ multilayers.

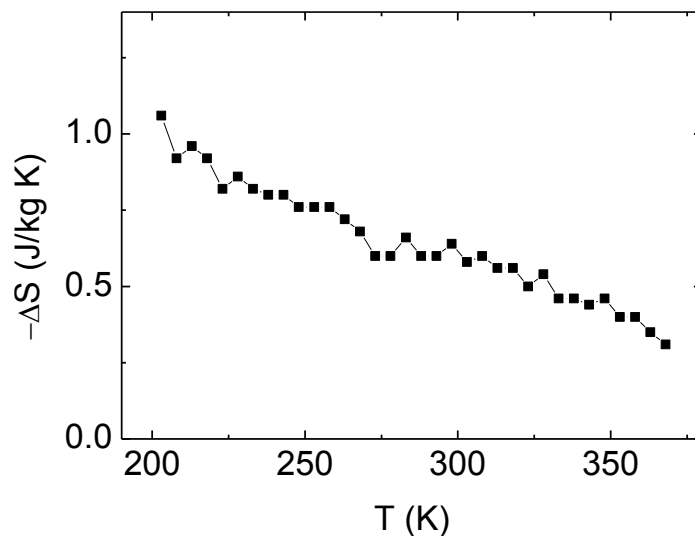


Figure 8. Temperature dependence of magnetic entropy change for the [Tb-Co(6 nm)/Si(2 nm)]₂₀ multilayers. $\Delta H = 7$ T.

4. Conclusion

Magnetocaloric effect of TbCo-based multilayers with different thickness of Tb-Co components and different kind of material of non-magnetic spacers was investigated. It was found that nanostructuring causes an increase in the width of the maximum temperature dependence of the magnetic entropy ΔS_M . Despite the reduction in the magnitude of this maximum, for the Ericsson-type magnetic refrigerators constant-induced magnetic entropy change as a function of temperature over the required operating range it is desirable. It has been established that the material of non-magnetic interlayers can have a noticeable effect on the MCE. In particular, silicon leads to a strong decrease in ΔS_M .

Acknowledgements

This work was supported by RFBR grant 17-02-00236-a of Russian Federation and by ELKARTEK ACTIMAT-3 (2018-19) KK-2018/00099 grant of the Basque Country Government.

References

- [1] Gschneidner K A, Jr. and Pecharsky V K 2000 *Annu. Rev. Mater. Sci.* **30** 387
- [2] Smaili A and Chahine R 1997 *J. Appl. Phys.* **81** 824
- [3] Niemann R, Heczko O, Schultz L and Fähler S 2010 *Appl. Phys. Lett.* **97** 222507
- [4] Kirby H F, Belyea D D, Willman J T and Miller C W 2013 *J. Vac. Sci. Technol. A* **31** 031506
- [5] Mansanares A M, Gandra F C G, Soffner M E, Guimarães A O, da Silva E C, Vargas H and Marin E 2013 *J. Appl. Phys.* **114** 163905
- [6] Shinde K P, Sinha B B, Oh S S, Kim H S, Ha H S, Baik S K, Chung K C, Kim D S and Jeong S 2015 *J. Magn. Magn. Mater.* **374** 144
- [7] Kirby B J, Lau J W, Williams D V, Bauer C A and Miller C W 2011 *J. Appl. Phys.* **109** 063905
- [8] Lambert C H, El Hadri M S, Hamedoun M, Benyoussef A, Mounkachi O and Mangin S 2017 *J. Magn. Magn. Mater.* **443** 1
- [9] Wang Z W, Yu P, Cui Y T and Xia L 2016 *J. Alloy Compd.* **658** 598
- [10] Tadout M, Lambert C-H, El Hadri M S, Mounkachi O, Benyoussef A, Hamedoun M, Benaissa M and Mangin S 2018 *J. Appl. Phys.* **123** 053902
- [11] Miller C W, Belyea D D and Kirby B J 2014 *J. Vac. Sci. Technol. A* **32** 040802
- [12] Svalov A V, Adanakova O A, Vas'kovskiy V O, Balymov K G, Larrañaga A, Kurlyandskaya G V, Domingues Della Pace R and Plá Cid C C 2018 *J. Magn. Magn. Mater.* **459** 57
- [13] Svalov A V, Vas'kovskiy V O, Lepalovskij V N, Larrañaga A and Kurlyandskaya G V 2018 *J. Magn. Magn. Mater.* **465** 147

- [14] Doblas D, Moreno-Ramírez L M, Franco V, Conde A, Svalov A V and Kurlyandskaya G V 2017 *Mater. Design* **114** 214
- [15] Hansen P, Clausen C, Much G, Rosenkranz M and Witter K 1898 *J. Appl. Phys.* **66** 756
- [16] Yeung I, Roshko R M and Williams G 1986 *Phys. Rev. B* **34** 3456
- [17] Pecharsky V K and Gschneidner K A, Jr 1999 *J. Appl. Phys.* **86** 565
- [18] Halder M, Yusuf S M, Mukadam M D and Shashikala K 2010 *Phys. Rev. B* **81** 174402
- [19] Franco V and Conde A 2012 *Scr. Mater.* **67** 594
- [20] Vas’kovskiy V O, Patrin G S, Velikanov D A, Svalov A V, Savin P A, Yuvchenko A A and Shchegoleva N N 2007 *Phys. Solid State* **49** 302